Practical approach to facilitate photovoltaic integration in distribution systems

Jalil Yaghoobi, Nadarajah Mithulananthan, Tapan Kumar Saha

School of ITEE, The University of Queensland, Brisbane, QLD 4067, Australia
E-mail: j.yaghoobi@uq.edu.au

Published in *The Journal of Engineering*; Received on 24th February 2016; Accepted on 26th February 2016

Abstract: Photovoltaic (PV) power is a promising source of renewable energy, which could satisfy a large portion of the authors' electricity needs. In order to achieve this, a high penetration of PV is required as it is limited in plant factor and its characteristics are completely different from the conventional generators. However, high penetration level might cause some problems for the network operation. One of the potential setbacks that have been widely reported by power utilities is a voltage rise due to reverse power flow. Considering this burning problem, this study develops a practical method based on power flow formulation. In this method, two matrices are derived for estimating the effect of PV real and reactive power injections on the system voltage profile. These simple scalar matrices are then applied to find the voltage sensitive buses and the optimum location and sizing for power compensation devices to improve the penetration level of PV. Comparison between actual and estimated results for IEEE 37-bus test system justifies the validity of proposed method for these applications.

1 Introduction

By the end of 2014 global photovoltaic (PV) installation has exceeded 178 GW [1]. Many of the installations are at distribution level in the form of rooftop PV units. This trend is expected to continue in the near future due to many economic, environmental and social benefits. However, it might cause some severe problems at the same time. Some of the major concerns of high PV penetration have been mentioned in [2–8]. In [2], problems of voltage oscillation and transient over-voltage after faults, and high voltage in sub transmission and distribution networks have been discussed. The authors in [3] have mentioned that high PV penetration might cause grid instability, additional power flow in transmission system, and reverse power flow in distribution system. Voltage variations in an unbalanced distribution system caused by PV power drop due to moving clouds have been studied in [8]. Reverse power flow could happen as a result of high generation of PV power during low load condition and could result in voltage exceeding beyond the allowable limit. This problem and possible solutions have been investigated in [4–7] for Australian context, and worldwide in [8–13]. It has been mentioned in [4] that some utilities have reported voltage rise problem in Australian distribution networks due to rapidly rising PV penetration. In [5], PV inverter tripping due to over-voltage has been noted by some distribution network providers in Australia as a common occurrence. According to [6] new PV installation is limited in some areas in Western Australia due to voltage rise problem.

Few of the key solutions to overvoltage problem are reactive power support from either PV or other sources, tap control of substation transformer, storage devices and load shaving [9–14]. Applying a volt/var control system, reactive power absorption by PV has been proposed in [9] to keep the voltage within network limits. Similarly control of PV reactive power by an adaptive control method has been studied in [10] to minimise the voltage variations and power losses in a radial distribution system. The authors in [11] have proposed a coordinated control of operation of on-load tap changer (OLTC) and charging and discharging of storage system to shave the peak load and reduce the stress on OLTC. In [13], optimal sizing and location of static VAR compensator devices to improve voltage profile in a distribution system with PV and wind power generation has been investigated. A control approach for storage devices has been proposed in [14] to alleviate the PV voltage impact and support the load during peak time. Application of storage devices, however, has some practical concerns, which have been discussed in [15].

As it can be seen from the literature, distribution systems are likely to face overvoltage problem when increasing PV penetration. As a result, it is vital to measure the proximity of a system with high PV penetration to overvoltage and assess the requirement for compensation devices. In the next step, some optimisation problems need to be solved to find the best location and sizing of PV and compensation devices. The authors [16–18] tried to minimise power loss and improve voltage profile in distribution system by optimising PV and battery storage location and sizing using different methods. Reactive power injection from PV has been considered as an option in the formulation of their optimisation problem.

To assess the voltage effect of PV, voltage sensitivity of system to PV power injection needs to be evaluated. Application of Jacobian matrix for sensitivity analysis is well known for transmission system [19]. However, due to a wide range of R and X values of line segments and high R/X ratio, this method might not be suitable for distribution systems [20]. In [21], by formation of a matrix whose structure is only dependent on the network topology, different types of sensitivities are estimated. However, the proposed method is complicated and for the case of multi power sources there is a restriction of fixed voltage buses, which reduces the practicality of the method.

This paper proposes a comprehensive and practical method to assess the effect of PV real and reactive power injections on steady-state voltage profile of distribution systems. Unlike some similar studies, the proposed method is simple and requires only calculating two scalar matrices by running power flow several times. Once these scalar matrices are calculated, there is no need to recalculate them. They can then be used to estimate the voltage effect of PV power injection, even in large distribution systems. Observed linearity between power injection and voltage change in a two-bus system obtained from analytical results, is the idea of voltage change estimation by these scalar matrices. In order to show the accuracy and usefulness of the proposed method, it is evaluated in some practical applications like finding optimum location and sizing for compensation devices to allow maximum PV penetration. It is assumed that solar irradiation is uniform within the studied distribution network and it is possible to connect different sizes in different places.

In the following sections, the first foundation of the method is developed through analytical derivation for a two-bus test feeder. On the basis of the analytical outcomes an algorithm is then introduced to calculate a scalar matrix to estimate the voltage effect of PV in a large radial distribution system. Next, practical applications

doi: 10.1049/joe.2016.0031

of the estimation method are discussed. The accuracy of estimated results is examined using the IEEE 37-bus test system.

2 Load voltage in a two-bus system

In order to find the effect of PV power on the voltage profile of a distribution system, an equivalent two-bus system as shown in Fig. 1 is used to derive the voltage expression at the load bus.

For the system in Fig. 1, the voltage and power equations for the load bus can be expressed as given in the following equation

$$\begin{cases} V_{\mathrm{L}}\angle\beta = E - Z_s\angle\theta_s I \\ S_{\mathrm{L}}\angle\theta_{\mathrm{L}} = V_{\mathrm{L}}\angle\beta I^* \end{cases} \tag{1}$$

Substituting current in terms of other parameters in (1) yields (2) for the load voltage magnitude

$$V_{\mathrm{L}}^4 + V_{\mathrm{L}}^2(2Z_sS_{\mathrm{L}}\cos(\theta_{\mathrm{L}} - \theta_s) - E^2) + Z_s^2S_{\mathrm{L}}^2 = 0 \tag{2}$$

In practical networks $Z_S \ll 1$ pu, while source voltage (E) and load power (S_{L}) are close to 1 pu; consequently $Z_sS_{\mathrm{L}} \ll E^2$. On the other hand, estimation $\sqrt{1+x} \cong 1 + 0.5x$ is valid for $|x| \ll 1$. Applying this estimation to the solution of (2) yields the simplified solution as given in the following equation

$$V_{\mathrm{L}} \cong E - \frac{R_sP_{\mathrm{L}} + X_sQ_{\mathrm{L}}}{E} - \frac{\left(R_sQ_{\mathrm{L}} - X_sP_{\mathrm{L}}\right)^2}{2E^3} \tag{3}$$

where R_s and X_s are real and imaginary parts of Z_s, respectively and P_{L} and Q_{L} are real and reactive parts of S_{L}, respectively.

2.1 Effect of PV power on the load voltage

In the next step, PV power of $S_{\mathrm{i}}\angle\theta_{\mathrm{i}}$ is injected to the load bus of the two-bus system. In this condition, the second part of (1) is modified as given in the following equation

$$S_{\mathrm{L}}\angle\theta_{\mathrm{L}} - S_{\mathrm{i}}\angle\theta_{\mathrm{i}} = V_{\mathrm{L}}\angle\beta I^* \tag{4}$$

With similar calculations and simplifications, the load voltage can be estimated as given in the following equation

$$\begin{aligned} V_{\mathrm{L}} \cong E &- \frac{1}{E}\left(R_sP_{\mathrm{L}} + X_sQ_{\mathrm{L}}\right) + \frac{1}{E}\left(R_sP_{\mathrm{i}} + X_sQ_{\mathrm{i}}\right) \\ &- \frac{1}{2E^3}\left(R_sQ_{\mathrm{L}} - X_sP_{\mathrm{L}}\right)^2 - \frac{1}{2E^3}\left(R_sQ_{\mathrm{i}} - X_sP_{\mathrm{i}}\right)^2 \\ &+ \frac{1}{E^3}\left(R_sQ_{\mathrm{L}} - X_sP_{\mathrm{L}}\right)\left(R_sQ_{\mathrm{i}} - X_sP_{\mathrm{i}}\right) \end{aligned} \tag{5}$$

where P_{i} and Q_{i} are real and reactive parts of injected PV power, respectively. Subtraction of (5) by (3) yields (6) for the voltage change induced by only PV power. That is, the change of voltage when the load is assumed to be the same before and after PV power injection

$$\begin{aligned} \Delta V_{\mathrm{L}} = &\frac{1}{E}\left(R_sP_{\mathrm{i}} + X_sQ_{\mathrm{i}}\right) - \frac{1}{2E^3}\left(R_sQ_{\mathrm{i}} - X_sP_{\mathrm{i}}\right)^2 \\ &+ \frac{1}{E^3}\left(R_sQ_{\mathrm{L}} - X_sP_{\mathrm{L}}\right)\left(R_sQ_{\mathrm{i}} - X_sP_{\mathrm{i}}\right) \end{aligned} \tag{6}$$

In this equation, with practical assumptions of small values for R_S and X_S, the second and third terms can be neglected compared to the first one. Therefore, the change in the voltage can be estimated by the following equation

$$\Delta V_{\mathrm{L}} \cong \frac{1}{E}\left(R_sP_{\mathrm{i}} + X_sQ_{\mathrm{i}}\right) \tag{7}$$

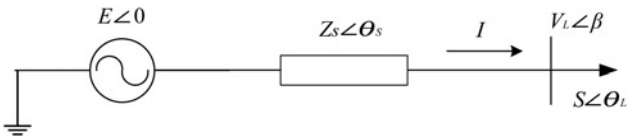

Fig. 1 *Equivalent two-bus power system used to measure the load voltage*

It should be noted that (7) is not valid in some extreme conditions like an injection of only reactive power (Q_{i}) to a pure resistive network ($X_s \cong 0$) or an injection of only real power (P_{i}) to a pure reactive network ($R_s \cong 0$). As these are not real world cases, (7) can be applied for practical systems.

2.2 Comparing results with Jacobian matrix

Inverse Jacobian matrix of the system can be used to calculate the change of phase angle and voltage magnitude as given in the following equation

$$\begin{bmatrix} \Delta\beta \\ \Delta V_{\mathrm{L}} \end{bmatrix} = \begin{bmatrix} \frac{\partial P_{\mathrm{L}}}{\partial\beta} & \frac{\partial P_{\mathrm{L}}}{\partial V_{\mathrm{L}}} \\ \frac{\partial Q_{\mathrm{L}}}{\partial\beta} & \frac{\partial Q_{\mathrm{L}}}{\partial V_{\mathrm{L}}} \end{bmatrix}^{-1} \begin{bmatrix} \Delta P_{\mathrm{L}} \\ \Delta Q_{\mathrm{L}} \end{bmatrix} \tag{8}$$

Using (8), the following relationship holds between ΔV_{L}, ΔP_{L} and ΔQ_{L}.

$$\Delta V_{\mathrm{L}} = -\left(\frac{Z_S\cos\left(\theta_S + \beta\right)}{2V_{\mathrm{L}}\cos\beta - E}\right)\Delta P_{\mathrm{L}} - \left(\frac{Z_S\sin\left(\theta_S + \beta\right)}{2V_{\mathrm{L}}\cos\beta - E}\right)\Delta Q_{\mathrm{L}} \tag{9}$$

By estimating $V_{\mathrm{L}} = (1-\varepsilon)E$, $\cos\delta \cong 1$ and $\sin\delta \cong \delta$ for practical assumption of ε, $\delta \ll 1$, (9) can be rewritten as given in the following equation

$$\begin{aligned} \Delta V_{\mathrm{L}} = &-\left(\frac{R_S\Delta P_{\mathrm{L}} + X_S\Delta Q_{\mathrm{L}}}{E}\right) + \beta\left(\frac{R_S\Delta Q_{\mathrm{L}} - X_S\Delta P_{\mathrm{L}}}{E}\right) \\ &+ 2\delta\left(\frac{R_S\Delta P_{\mathrm{L}} + X_S\Delta Q_{\mathrm{L}}}{E}\right) - 2\delta\beta\left(\frac{R_S\Delta Q_{\mathrm{L}} - X_S\Delta P_{\mathrm{L}}}{E}\right) \end{aligned} \tag{10}$$

ΔV_{L} can be estimated by the first term of (10), which is the same as (7) when $\Delta P_{\mathrm{L}} = -P_{\mathrm{i}}$ and $\Delta Q_{\mathrm{L}} = -Q_{\mathrm{i}}$. Consequently, similar results for the first-order estimation were calculated using Jacobian matrix of the system. Equation (7) shows two important aspects of voltage change by PV power. First, while V_{L} clearly depends on the amount of existing load (S_{L}), ΔV_{L} is almost independent from this value and is mainly identified by the line characteristics (R_S and X_S) and injected PV power (P_{i} and Q_{i}). Second, ΔV_{L} shows a linear relationship with injected PV power. Considering these features, (7) can be rewritten as given in the following equation

$$\Delta V_{\mathrm{L}} \cong k_pP_{\mathrm{i}} + k_qQ_{\mathrm{i}} \tag{11}$$

where $k_p = R_S/E$ and $k_q = X_S/E$ are nearly constant coefficients relating the voltage rise to power injection. This equation will be extended to the general case of a multi-bus system in the following section.

3 Voltage effect of PV in a multi-bus system

Acquired results in the previous section are valid for a two-bus system with only one load bus. However, the linear relationship between voltage change and injected power in (11) might exist in a multi-bus system. With this assumption, the relationship

between voltage change at each bus and injected P and Q to that bus and other buses can be estimated by scalar coefficients. Therefore, two scalar matrices of $\boldsymbol{K}_P$ and $\boldsymbol{K}_Q$ are defined to describe this linear relationship in an n-bus system as given in the following equation

$$\begin{bmatrix} \Delta V_1 \\ \vdots \\ \Delta V_n \end{bmatrix} = \begin{bmatrix} k_{11P} & \cdots & k_{1nP} \\ \vdots & \ddots & \vdots \\ k_{n1P} & \cdots & k_{nnP} \end{bmatrix} \begin{bmatrix} P_1 \\ \vdots \\ P_n \end{bmatrix} + \begin{bmatrix} k_{11Q} & \cdots & k_{1nQ} \\ \vdots & \ddots & \vdots \\ k_{n1Q} & \cdots & k_{nnQ} \end{bmatrix} \begin{bmatrix} Q_1 \\ \vdots \\ Q_n \end{bmatrix} \tag{12}$$

where k_{ijP} and k_{ijQ} are used to relate the effect of P_j and Q_j (active and reactive PV power values injected to bus j) on the voltage of bus i. Likewise, ΔV_i is the voltage change of bus i induced by all P and Q injections. It should be mentioned that ΔV in (12) is only due to the PV power injection and not the load change. The effect of load change, however, can be easily estimated by (12) by assuming P_j and Q_j as the net power injection (PV power subtracted by load power change).

In order to calculate n^2 elements of $\boldsymbol{K}_P$ and $\boldsymbol{K}_Q$ the following steps should be carried out:

(i) $P_i = P_{\text{test}}$ is injected to bus i while no P and Q are injected to other buses.
(ii) Using power flow, the change in voltage profile of the system (ΔV_1, …, ΔV_n) by this power injection is calculated.
(iii) Elements of the ith column are calculated using the following equation

$$\begin{bmatrix} k_{1iP} \\ \vdots \\ k_{niP} \end{bmatrix} = \begin{bmatrix} \Delta V_1/P_{\text{test}} \\ \vdots \\ \Delta V_n/P_{\text{test}} \end{bmatrix} \tag{13}$$

By implementing this algorithm for all buses (n times), all the elements of $\boldsymbol{K}_P$ are determined. Similarly, $\boldsymbol{K}_Q$ can be calculated by first injecting a Q_{test} to each bus, then measuring voltage rises to find the elements of the ith column of $\boldsymbol{K}_Q$ using the following equation

$$\begin{bmatrix} k_{1iQ} \\ \vdots \\ k_{niQ} \end{bmatrix} = \begin{bmatrix} \Delta V_1/Q_{\text{test}} \\ \vdots \\ \Delta V_n/Q_{\text{test}} \end{bmatrix} \tag{14}$$

This algorithm shows that $\boldsymbol{K}_P$ and $\boldsymbol{K}_Q$ can easily be determined for even large systems. However, the accuracy of estimation results by these matrices needs to be validated. For that purpose, the estimated results have been compared with actual power flow results of the IEEE 37-bus system in Section 5. It has been observed that estimated results follow the actual outcomes with an acceptable error in a practical range of PV power injection. Taking into account this justification, potential applications of the proposed estimation method are investigated in the following section.

4 Applications of the estimation method

Compared to other methods, the proposed estimation method is a simple method for voltage sensitivity analysis of distribution systems. The main advantage of this method is that it only needs to calculate two scalar matrices. These scalar matrices can easily be calculated by running power flow for $2 \times n^2$ times for an n-bus system. They can then be used to measure the voltage change by PV power injection without the requirement for recalculation. Consequently, the proposed estimation method is a simple and practical analysis tool to evaluate the influence of PV power injection on the voltage of any distribution network. Some potential applications of the proposed estimation method including identifying sensitive buses to power injection, maximum PV penetration level and optimum location and sizing of compensation devices are described as follows.

4.1 Identifying sensitive buses

As can be seen from (12), elements of $\boldsymbol{K}_P$ and $\boldsymbol{K}_Q$ directly relate voltage change to injected power. As a result, comparison between magnitudes of these elements shows whether injecting P is more effective to control the voltage or Q; that is, the voltage influence of the power (P or Q) related to the matrix with larger elements is higher. Besides, considering (7), elements of $\boldsymbol{K}_P$ mainly depend on line resistance whereas elements of $\boldsymbol{K}_Q$ are more related to line reactance. As a result, elements of $\boldsymbol{K}_P$ are predicted to be higher in a distribution system with $R/X > 1$ and voltage effect of injecting P is predicted to be more than Q. Within each matrix, a large element shows high voltage sensitivity to power injection in the corresponding bus. If the large element is diagonal (k_{ii}), bus i voltage is highly sensitive to injected power to itself, whereas a large off-diagonal element (k_{ij}) shows high voltage sensitivity of bus i to power injected to bus j. In this way, large elements on ith row represent the buses to which power injection highly affects the bus i voltage.

4.2 Optimum location and sizing of compensation devices

Knowing that it is not usually feasible to have a strict control over the location and sizing of PV units in a distribution system, a practical solution to improve the maximum allowable PV generation is utilising power compensation devices. During high generation of PV power, storage and reactive power compensation devices can mitigate the overvoltage by absorbing real and reactive power values. In order to find the best location and sizing of these devices, the proposed estimation method can be utilised. On the basis of the requirements of power compensation devices, different scenarios have been considered to find their best location and sizing, which are discussed as follows. It should be noted that these scenarios only discuss storage devices with real power capabilities. However, a similar method can be used for reactive power compensation devices.

4.2.1 Maximising storage voltage effects (SVEs): In this research, the sum of all the voltage effects in the system by a storage device of 1 pu connected to bus j is defined as storage voltage effect of the bus j. To find the location of the highest SVE, assume that a storage system absorbing $P_{\text{bat}} = 1$ pu (or injecting $-P_{\text{bat}} = -1$ pu) is connected to bus j. Using (12), the total amount of voltage drops at all buses caused by charging the battery at bus j can be obtained from the following equation

$$\sum_{i=1}^{n} \Delta V_i = -\left(\sum_{i=1}^{n} k_{Pij}\right) P_{\text{bat}} = -\left(\sum_{i=1}^{n} k_{Pij}\right) \tag{15}$$

It can be deduced from (15) that SVE of the storage at bus j equals to $\sum_{i=1}^{n} k_{Pij}$, which is the sum of the elements of the column j of $\boldsymbol{K}_P$. Consequently, after calculating this sum for all columns, the bus corresponding to the maximum value has the highest SVE and should be selected for connecting the storage device if the highest voltage effect from it is desired. It is worth mentioning that selecting the location with the highest SVE is recommended when the system operation with PV units is normal and there is no overvoltage problem. In this case, selecting the location with the highest SVE assures using maximum capacity of voltage control by the storage device. On the other hand, if the distribution system is experiencing overvoltage problems due to high PV power generation,

doi: 10.1049/joe.2016.0031

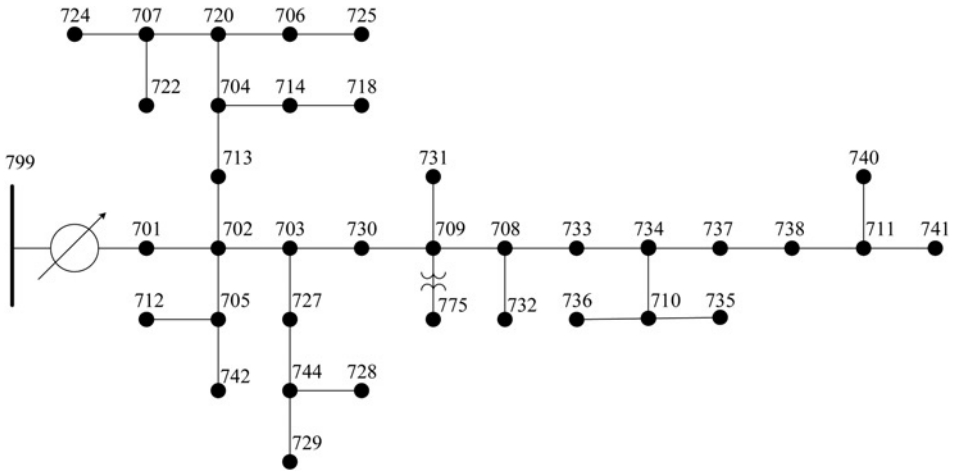

Fig. 2 *IEEE 37-bus radial distribution system [24]*

the priority of storage device allocation should be mitigating the overvoltage problem. This case is discussed as follows.

4.2.2 Optimum location and sizing of storage to mitigate the overvoltage problem: In this scenario, it is assumed that high PV power generation has caused overvoltage at some or all buses of the distribution system. As a result, an optimisation problem as given in (16) needs to be formulated to find optimum location and sizing of storage devices to mitigate the overvoltage problem

$$\begin{cases} \Delta V_{\text{comp},i} = \sum_{j=1}^{n} k_{Pij} P_{\text{comp},j} \geq \Delta V_{\text{viol},i} \\ 0 \leq P_{\text{comp},i} \leq P_{\text{comp, max}} \end{cases} \quad (i = 1, \ldots, n) \tag{16}$$

where $\Delta V_{\text{comp},i}$ is the voltage drop at bus i caused by all storage units of $P_{\text{comp},j}(j = 1{:}n)$ and $\Delta V_{\text{viol},i}$ is the voltage violation at bus i due to high generation of PV power. $P_{\text{comp,max}}$ is the maximum available size of storage devices. If utility sized storage devices are used, another limit will be the number of devices, which in a real situation might be as low as one or two units for a typical distribution system.

4.2.3 Storage device index (SDI): The minimum requirement of a storage device to compensate the voltage effect of PV units can be represented by an index called storage device index in this research. After finding the best location for the storage device, this index can be used to find its minimum required size. In order to explain this index, assume that PV units with a similar size of P_{PV} are connected to all the buses while a storage device is connected to bus k and absorbing $P_{\text{bat},k}$. For all the buses, voltage effect of $P_{\text{bat},k}$ needs to be higher than PV units to compensate their voltage impact. Using (12), this condition is formulated as the inequality given in the following equation

$$k_{Pik} P_{\text{bat},k} \geq \sum_{j=1}^{n} k_{Pij} P_{\text{PV}} \quad (i = 1, \ldots, n) \tag{17}$$

To assure that voltage effect of the storage device is always higher, $P_{\text{bat},k}$ has to be selected as given in the following equation

$$P_{\text{bat},k} = \max\left(\frac{\sum_{j=1}^{n} k_{Pij}}{k_{Pik}} P_{\text{PV}} \right) \quad (i = 1, \ldots, n) \tag{18}$$

where $P_{\text{bat},k}$ is the minimum requirement of the storage device power to guarantee the compensation of voltage effect of PV units in all the buses. Therefore, optimum location and minimum required $P_{\text{bat},k}$ can be obtained as given in the following equation

$$P_{\text{bat, min}} = \min\left(P_{\text{bat},k}\right) \quad (k = 1, \ldots, n) \tag{19}$$

where $P_{\text{bat,min}}$ is the minimum required size of the storage device and the corresponding bus is the optimum place. Finally, using (18) and (19), SDI is defined as given in the following equation

$$\begin{aligned} \text{SDI} &= P_{\text{bat, min}} / P_{\text{o}} \\ &= \min\left[\max\left(\frac{\sum_{j=1}^{n} k_{Pij}}{k_{Pit}} \right) \quad (i = 1, \ldots, n) \right] \\ &\quad (t = 1, \ldots, n) \end{aligned} \tag{20}$$

This index indicates the kilowatt amount of storage device required to compensate each kilowatt of uniformly distributed PV. These calculations, however, are only valid for the case of one storage device. If more than one storage device is available, an optimisation problem needs to be formulated and solved. SDI is further discussed for the case of the IEEE 37-bus test system in the following section.

5 Evaluation of the estimation method in the IEEE 37-bus system

In this section, the proposed estimation method is validated for the IEEE 37-bus distribution system [22] shown in Fig. 2, and its applications are investigated. This system has a rated load of 2.46 MW and 1.20 MVAr. It should be noted that in this section the average value of three phase voltages represents the voltage magnitude at each bus. Analytical software tool PSCAD [23] has been used to simulate this system and verify the proposed applications.

5.1 Accuracy of estimation results

Using the algorithm described in Section 3, $\boldsymbol{K}_P$ and $\boldsymbol{K}_Q$ were obtained for the IEEE 37-bus system. In order to calculate these matrices, $P_{\text{test}} = 600$ kW (200 kW to each phase) and $Q_{\text{test}} = 600$ kVAr (200 kVAr to each phase) were used. However, other values of test power values in practical ranges have shown to yield similar results. It should be noted that in this system, $\boldsymbol{K}_P$ and $\boldsymbol{K}_Q$ have dimensions of 25×25 to represent 25 active buses (load-connected buses). To validate the estimation results by these matrices, Fig. 3 compares estimated voltage changes at the active buses with actual values obtained from power flow for an arbitrary set of power injections with a high PV penetration level of 70% of rated load (1.7 MW and 0.9 MVAr).

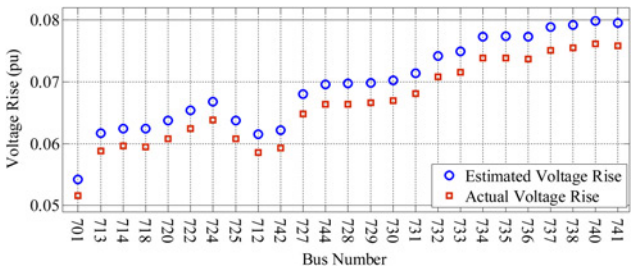

Fig. 3 *Voltage rise estimated by $\boldsymbol{K}_P$ and $\boldsymbol{K}_Q$ matrices and actual voltage rise from power flow in 25 active buses of IEEE 37-bus system*

Fig. 3 confirms there is a small error of less than 5% between estimated and actual values in all buses; that is, a reasonably accurate estimation of voltage change has been made by the proposed estimation method using $\boldsymbol{K}_P$ and $\boldsymbol{K}_Q$. It is worth mentioning that errors are even smaller for lower penetration levels. Fig. 3 also shows that the voltage rise in buses like 740, 741 and 738 is higher than buses like 701, 713 and 714. By looking at the IEEE 37-bus system in Fig. 2, it can be seen that the first three buses are close to the end of the feeder, while the later ones are close to the substation. Consequently, it can be deduced that distributed PV power generation in the system has a higher voltage impact in remote buses. This higher voltage impact can also be predicted by comparing the elements of $\boldsymbol{K}_P$ and $\boldsymbol{K}_Q$, as the elements related to buses close to the end of the feeder are generally larger than others. The larger elements in these matrices show higher voltage sensitivity to PV power injection.

Next, to validate the estimation method when both load and PV change during time, a typical summer load profile and PV generation curve from [25] have been used. In this case, Fig. 4 compares estimated and actual voltage changes at bus 741 for 70% PV penetration level.

Fig. 4 shows the estimated values of PV voltage effect closely follow actual values from power flow analysis. The load level shown in this figure has a large daily variation from around 1.3 to 2.5 MVA. Also, the PV power generation varies from small values in the early morning and late afternoon to around 1.7 MVA during peak power generation at midday. Small errors between estimated and actual voltage changes shown in Fig. 4 for this large variation in the system load and PV generation confirms the effectiveness of the estimation method. In other words, the proposed method can accurately predict voltage change using calculated matrices without a requirement for modifying these matrices. Similar accuracy has been observed for voltage change

Table 1 Voltage sensitive buses to P and Q injections determined by elements of $\boldsymbol{K}_P$ and $\boldsymbol{K}_Q$, and relative voltage rises

No.	P_{inj} = 300 kW			Q_{inj} = 300 kVA		
	Bus	k_{pii}	dV_{act}, pu	Bus	k_{qii}	dV_{act}, pu
1	736	13,838	0.0170	741	13,588	0.0167
2	724	11,900	0.0146	736	13,575	0.0167
3	741	11,313	0.0139	740	13,433	0.0165
4	740	11,308	0.0139	738	12,892	0.0158
5	735	10,567	0.0130	735	12,621	0.0154

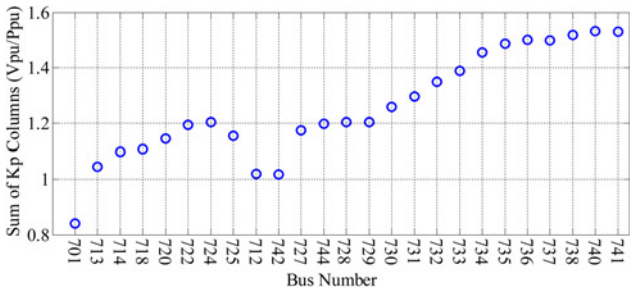

Fig. 5 *Column sums of $\boldsymbol{K}_P$ and corresponding buses*

at other buses. Therefore, the validity of application of the proposed method to estimate the voltage change by PV power is justified.

The validity of the estimation method confirms that PV power effect on the voltage profile mainly depends on the amount of injected power not the existing load of the system. To explain this, Fig. 4 shows the estimation method accurately predicts the voltage change by PV power injection at different load levels. On the other hand, as (12) shows, the method only uses values of PV power injection and scalar matrices to calculate voltage change and does not need the amount of existing load. Consequently, it is confirmed that the voltage change by PV power mainly depends on the amount of injected power and is almost independent of the existing system load for a multi-bus system like the IEEE 37-bus system. Next, the proposed applications of the estimation method are examined for this test system as follows.

5.2 *Identifying buses sensitive to power injection*

According to line characteristics of the IEEE 37-bus, the resistance of line segments is always higher than their inductive reactance.

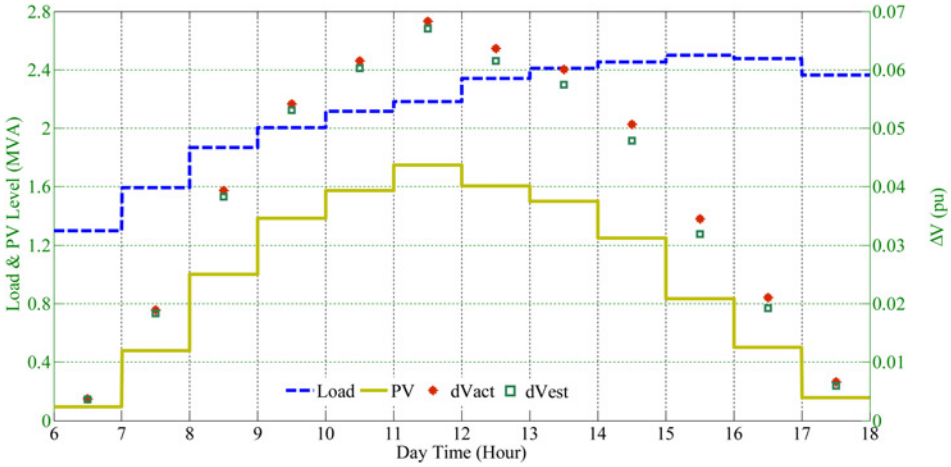

Fig. 4 *Comparison of estimated voltage rise with actual voltage rise for bus 741 for varying levels of load and PV*

Table 2 Voltage change in the system with PV units and one storage device compared to the base case

Bus	ΔV, pu	Bus	ΔV, pu	Bus	ΔV, pu	Bus	ΔV, pu	Bus	ΔV, pu
701	−0.0015	722	−0.0005	727	−0.0015	731	−0.0005	736	−0.0065
713	−0.0015	724	−0.0004	744	−0.0015	732	−0.0004	737	−0.00878
714	−0.0012	725	−0.0008	728	−0.0012	733	−0.0008	738	−0.0098
718	−0.0011	712	−0.0016	729	−0.0011	734	−0.0016	740	−0.0121
720	−0.0009	742	−0.0017	730	−0.0009	735	−0.0017	741	−0.0109

However, due to a high X/R ratio ($X = 0.08$ pu and $R = 0.02$ pu) of the substation transformer, the overall reactance of current paths is higher than the resistance. Consequently, $\boldsymbol{K}_Q$ has greater elements compared to $\boldsymbol{K}_P$. It means that Q injection is more effective than P injection on the voltage profile of the system. As was previously mentioned, larger elements in each matrix show higher voltage sensitivity to power injection. As an example of $\boldsymbol{K}_P$ of the IEEE 37-bus system, voltage sensitivity of bus 736 to P injection is four times higher than that of bus 701. Likewise, as can be seen from $\boldsymbol{K}_Q$ of this system, bus 736 is 1.6 times more voltage sensitive to Q injection than bus 701. This observation could be predicted from the difference in line impedances from the substation to these buses. As can be seen from Fig. 2, bus 701 is very close to the substation, whereas bus 736 is close to the end of the feeder. Similar assessments can be done for the sensitivity of other buses to power injection easily by comparing their corresponding values in $\boldsymbol{K}_P$ and $\boldsymbol{K}_Q$. Table 1 sorts the highest sensitive buses to P and Q injections obtained from these matrices. Along with sorted buses with the highest related k_{pii} and k_{qii} values, actual measured voltage changes by injecting 300 kW and 300 kVAr are shown to validate the arrangement.

This table justifies that remote buses are generally more voltage sensitive to power injection due to longer lines and higher impedances from the substation bus to the load bus. However, the sensitivity rankings of buses are different in P and Q injections. As an example, bus 741 shows the highest voltage sensitivity to Q injection, whereas in the ranking of voltage sensitivity to P injection, it is located in the third position after buses 736 and 724. Similarly, bus 738 has fourth place in the ranking of voltage sensitive buses to Q injection, whereas this bus is not part of five most voltage sensitive buses to P injection. Similar observations can be made for other buses. Consequently, as $\boldsymbol{K}_P$ and $\boldsymbol{K}_Q$ matrices predict and actual results confirm, buses have generally different P and Q voltage sensitivity when compared with other buses. Besides the observed difference in rankings, each bus has a different voltage sensitivity to P injection compared with Q injection. For example, k_{qii} for bus 735 is 12,621, whereas it has a k_{pii} of 10,567. That is, if similar amounts of P and Q are injected to this bus, voltage rise by Q injection will be around 19.4% higher. Table 1 shows the voltage rise in this bus by injecting $P = 300$ kW is 0.0130 pu, whereas injection of $Q = 300$ kVAr increases its voltage by 0.0154 pu. That is, 18.5% higher voltage rise by Q injection compared with P injection as was closely estimated by comparing k_{qii} and k_{pii}.

5.3 *Optimum location and sizing of storage devices*

Besides assessing the effect of PV power on the voltage profile of a distribution system, the estimation method can be used to identify the location and sizing of a storage device as was proposed in Section 4.2. It should be noted that the main objective for placement and sizing of storage devices considered in this research is its ability to absorb power to compensate the effect of high PV penetration.

5.3.1 Maximising SVE: In order to achieve the maximum SVE, the storage device must be connected to the bus corresponding to the column of $\boldsymbol{K}_P$ with the highest sum of elements. Column sums related to active buses of the IEEE 37-bus system, representing SVE values are shown in Fig. 5. As this figure shows, buses 741, 740 and 738 are the three best locations for connecting a storage device to achieve high voltage effects by storage devices. On the other hand, connecting the storage device to bus 701 will result in the lowest SVE. It can also be deduced from Fig. 5 that buses close to the end of the feeder generally have higher SVE and consequently are more effective options for adding an energy storage system. Due to this, SVE values of remote buses like 741, 740 and 738 are higher than 1.5 $V_{\text{pu}}/P_{\text{pu}}$, whereas this value is around 1 $V_{\text{pu}}/P_{\text{pu}}$ in buses close to the substation, like 712 and 742. In this way, connecting storage devices to remote buses shows more than 50% higher influence on the overall system voltage compared with buses close to the substation in the IEEE 37-bus system.

5.3.2 Assessing SDI: Using (20), SDI, which is the required kilowatt amount of storage device to compensate the effect of 1 kW of uniformly added PV, is calculated as 29.95 $\text{kW}_{\text{storage}}/\text{kW}_{\text{PV}}$. This value is for the scenario of one storage device, which must be

Table 3 SDI and optimum buses for the case of two storage devices

Bus	722	737	Total
SDI, kW/kW	5.92	19.36	25.28

Table 5 SDI and optimum buses for the case of three storage devices

Bus	720	744	737	Total
SDI, kW/kW	7.50	1.49	16.07	25.06

Table 4 Voltage change in the system with PV units and two storage devices compared to the base case

Bus	ΔV, pu	Bus	ΔV, pu	Bus	ΔV, pu	Bus	ΔV, pu	Bus	ΔV, pu
701	−0.0002	722	−0.0012	727	−0.0003	731	−0.0012	736	−0.0022
713	−0.0002	724	−0.0009	744	−0.0002	732	−0.0015	737	−0.0036
714	−0.0002	725	−0.0003	728	−0.0001	733	−0.0019	738	−0.0035
718	−0.0001	712	−0.0002	729	−0.0001	734	−0.0026	740	−0.0034
720	−0.0004	742	−0.0002	730	−0.0010	735	−0.0024	741	−0.0034

Table 6 Voltage change in the system with PV units and three storage devices compared to the base case

Bus	ΔV, pu	Bus	ΔV, pu	Bus	ΔV, pu	Bus	ΔV, pu	Bus	ΔV, pu
701	−0.00011	722	−0.00016	727	−0.00019	731	−0.00069	736	−0.00130
713	−0.00018	724	−0.00003	744	−0.00011	732	−0.00091	737	−0.00254
714	−0.00023	725	−0.00042	728	−0.00006	733	−0.00129	738	−0.00242
718	−0.00013	712	−0.00004	729	−0.00005	734	−0.00176	740	−0.00230
720	−0.00053	742	−0.00005	730	−0.00061	735	−0.00152	741	−0.00230

connected to bus 741. It means that if 1 kW of PV is injected to all the active buses, a battery unit with the size of 29.95 kW at bus 741 is needed as the minimum requirement to compensate the voltage effect of PV units. In order to check the accuracy of this value, PV units of 15 kW are connected uniformly to 25 active buses while a storage device of $29.95 \times 15 = 449.25$ kW is absorbing power at bus 741. In this scenario, Table 2 shows the voltage change in all the buses compared to the base case with no PV and no storage.

This table shows that for all buses $\Delta V < 0$; that is, voltage rise by PV units is completely compensated by the storage device. Moreover, voltage reduction in buses close to bus 741 is higher as the storage device is connected to this bus. If more than one storage device is intended to be used, an optimisation problem should be defined and solved to obtain the minimum requirement of storage devices. For scenarios of two and three storage devices, best locations and their corresponding SDIs are discussed as follows. For the case of using two storage devices, these parameters are obtained as presented in Table 3.

Compared to the case of a single storage device, this case shows 15.6% reduction in SDI value (25.28 against 29.95). This shows that less total storage amount is required when two units are used instead of one. Furthermore, the best location for connecting the storage devices is different to the previous case. That is, whereas the best bus to connect one storage device is bus 741, when two devices are utilised the best buses are 722 and 737. Therefore, one important parameter for the best location and sizing of storage devices is the number of devices that are going to be deployed. In order to justify the validity of acquired results, two storage devices of $15 \times 5.92 = 88.8$ kW and $15 \times 19.36 = 290.4$ kW are connected to buses 722 and 737, respectively. PV units of 15 kW are also connected uniformly in all the buses. In this condition, Table 4 shows the voltage change of the system compared to the base case.

According to this table, as for all buses $\Delta V < 0$, storage devices have completely mitigated the voltage rise by PV units. Consequently, it is confirmed that when two storage devices are used to mitigate the voltage effect of PV power units, less total value is required compared with the case of one storage device. In the next step, three storage units are assumed to be utilised. In this scenario, optimum locations and corresponding SDIs are calculated as given in Table 5.

This table shows that SDI in this scenario is 16.3% smaller than the scenario of using a single storage device. As a result, a lower amount of storage is required to compensate the voltage effect of PV. Table 6 shows the voltage change between the base case and the case with uniform 15 kW PV units and three storage units with sizes $7.50 \times 15 = 112.5$ kW, $1.49 \times 15 = 22.35$ kW and $16.07 \times 15 = 241.05$ kW connected to buses 720, 744 and 737, respectively.

Negative values for ΔV in Table 6 confirm the effectiveness of proposed storage devices to alleviate the voltage rise by PV. It should be noted that comparing SDI values in this case with the case using two storage devices only shows a slightly (0.9%) less total storage requirement. That is, adding the complexity and cost of utilising three storage devices instead of two does not reduce the total storage requirement. This implies that between three studied options for the number of storage devices, the best option could be using two storage devices as it shows some reduction in required total size compared with the single storage case. However, due to higher possible cost and technical complexity of using two storage devices compared with a single device, the selection between these two options needs a thorough comparison between economic and technical factors.

As can be seen from the results in this section, using the proposed estimation method, best location and sizing for storage devices can be easily obtained. Similar procedures can be followed for utilising reactive power compensation devices. The only difference is to find the voltage effect of reactive power compensation devices, $\boldsymbol{K}_Q$ matrix is utilised instead of $\boldsymbol{K}_P$. Overall, the voltage change estimation results obtained by the proposed estimation method were accurate when evaluated in the IEEE 37-bus distribution system. Furthermore, the proposed estimation method showed its potential applications for optimisation studies of PV and storage allocation and sizing.

6 Conclusions

To facilitate high penetration of PV units in distribution systems, this paper establishes an estimation method. The method captures voltage impact due to PV power injection and helps identifying sensitive locations and sizes of compensation devices to facilitate maximum PV penetration. The method was tested in IEEE 37-bus test distribution system. Results for this system confirm that the method predicts voltage effect of PV with a satisfactory accuracy when compared with actual results. Moreover, this method is applied for identifying voltage sensitive buses and location and sizing of compensation devices, including energy storage, to mitigate the voltage rise by PV and maximise the PV penetration level in the test system. The numerical results for various applications demonstrate the usefulness of the method.

7 Acknowledgment

The authors thankfully acknowledge Australian Research Council (ARC) and Ingenero for providing supports for this work.

8 References

[1] 'Global Market Outlook for Solar Power 2015-2019', (Solar Power Europe, 2015), available online at http://www.solarpowereurope.org/insights/global-market-outlook/
[2] Zhang Y., Zhu S., Sparks R., Green I.: 'Impacts of solar PV generators on power system stability and voltage performance'. IEEE Power and Energy Society General Meeting (PESGM), 2012
[3] Appen J.V., Braun M., Stetz T., Diwold K., Geibel D.: 'Time in the sun', *IEEE Power Energy Mag.*, 2013, **11**, (2), pp. 55–64
[4] 'PV in Australia 2012', (Australian PV Association, 2013)
[5] 'PV integration on Australian distribution networks', (The Australian PV Association, 2013)
[6] 'Solar intermittency: Australia's clean energy challenge', (CSIRO, 2012)
[7] Guinane A., Shafiullah G.M., Oo A.M.T., Harvey B.E.: 'Voltage fluctuations in PV penetration on SWER networks – a case study for regional Australia'. IEEE Power and Energy Society General Meeting (PESGM), 2012
[8] Yan R., Saha T.K.: 'Voltage variation sensitivity analysis for unbalanced distribution networks due to photovoltaic power fluctuations', *IEEE Trans. Power Syst.*, 2012, **27**, (2), pp. 1078–1089

[9] Jahangiri P., Aliprantis D.C.: 'Distributed Volt/VAr control by PV inverters', *IEEE Trans. Power Syst.*, 2013, **28**, (3), pp. 3429–3439
[10] Yeh H.G., Gayme D.F., Low S.H.: 'Adaptive VAR control for distribution circuits with photovoltaic generators', *IEEE Trans. Power Syst.*, 2012, **27**, (3), pp. 1656–1663
[11] Liu X., Aichhorn A., Liu L., Li H.: 'Coordinated control of distributed energy storage system with tap changer transformers for voltage rise mitigation under high photovoltaic penetration', *IEEE Trans. Smart Grid*, 2012, **3**, (2), pp. 897–906
[12] Keane A., Ochoa L.F., Vittal E., Dent C.J., Harrison G.P.: 'Enhanced utilization of voltage control resources with distributed generation', *IEEE Trans. Power Syst.*, 2011, **26**, (1), pp. 252–260
[13] Savić A., Đurišić Ž.: 'Optimal sizing and location of SVC devices for improvement of voltage profile in distribution network with dispersed photovoltaic and wind power plants', *Appl. Energy*, 2014, **134**, pp. 114–124
[14] Alam M.J.E., Muttaqi K.M., Sutanto D.: 'Mitigation of rooftop solar PV impacts and evening peak support by managing available capacity of distributed energy storage systems', *IEEE Trans. Power Syst.*, 2013, **28**, (4), pp. 3874–3884
[15] Parra D., Gillott M., Norman S.A., Walker G.S.: 'Optimum community energy storage system for PV energy time-shift', *Appl. Energy*, 2015, **137**, pp. 576–587
[16] Hung D.Q., Mithulananthan N., Bansal R.C.: 'Analytical strategies for renewable distributed generation integration considering energy loss minimization', *Appl. Energy*, 2013, **105**, pp. 75–85
[17] Hung D.Q., Mithulananthan N., Bansal R.C.: 'Integration of PV and BES units in commercial distribution systems considering energy loss and voltage stability', *Appl. Energy*, 2014, **113**, pp. 1162–1170
[18] Fu X., Chen H., Cai R., Yang P.: 'Optimal allocation and adaptive VAR control of PV-DG in distribution networks', *Appl. Energy*, 2015, **137**, pp. 173–182
[19] Kundur P.: 'Power system stability and control' (McGraw-Hill, 1994, 1st edn.)
[20] Haque M.H.: 'Efficient load flow method for distribution systems with radial or meshed configuration', *Proc. Inst. Elect. Eng., Gener. Transm. Distib.*, 1996, **143**, (1), pp. 33–38
[21] Khatod D.K., Pant V., Sharma J.: 'A novel approach for sensitivity calculations in the radial distribution system', *IEEE Trans. Power Deliv.*, 2006, **21**, (4), pp. 2048–2057
[22] Kersting W.H.: 'Radial distribution test feeders'. IEEE Power Engineering Society Winter Meeting, 2001, vol. 2, pp. 908–912
[23] PSCAD: https://www.hvdc.ca/pscad/
[24] IEEE 37-bus test system: http://www.ewh.ieee.org/soc/pes/dsacom/testfeeders/
[25] Load and PV data: http://www.aemo.com.au/Electricity/